Exploiting tube high-pressure shearing to prepare a microstructure in Pb-Sn alloys for unprecedented superplasticity

Kui Lin[a,#], Zheng Li[a,#], Ying Liu[a], En Ma [b,*], Jing Tao Wang[a,*], Terence G. Langdon[c]

[a] School of Materials Science and Engineering, Nanjing University of Science & Technology, Nanjing 210014, China
[b] Center for Alloy Innovation and Design (CAID), State Key Laboratory for Mechanical Behavior of Materials, Xi'an Jiaotong University, Xi'an 710049, China
[c] Materials Research Group, Department of Mechanical Engineering, University of Southampton, Southampton SO17 1BJ, U.K.

[#] Co-first authors, Kui Lin, linkui@njust.edu.cn
Zheng Li, lizheng@njust.edu.cn
[*] Co-corresponding authors, Jing Tao Wang, jtwang@njust.edu.cn
En Ma, maen@xjtu.edu.cn

Abstract

Superplastic Pb-Sn alloys were produced via tube high-pressure shearing (*t*-HPS), in a single step starting from elemental solids. A Pb-40 wt% Sn alloy showed an exceptional superplastic elongation as high as ~1870% at a strain rate of 1.0×10^{-3} s^{-1} at room temperature, thereby elevating the optimum strain rate for maximum elongation under these conditions by more than one order of magnitude over conventional cast Pb-Sn alloys. This unprecedented room temperature superplasticity is attributed to the equiaxed grains having uniform sizes of the order of one micrometer, and in particular to the well-mixed domains of Pb and Sn in nearly equal proportions. This microstructure cannot be attained in cast eutectic or hypoeutectic alloys through conventional thermomechanical processing, but instead it is a direct outcome of *t*-HPS-generated compositional patterning at room temperature.

Keywords: Compositional patterning; Pb-Sn alloys; severe plastic deformation; superplasticity; tube high-pressure shearing.

The development of superior mechanical properties in a material demands the production of highly refined grains and phases within the internal microstructure. This is especially true for achieving superplasticity, which is the ability of a material to elongate to more than 400% plastic strain in tensile deformation [1]. An extensive uniform elongation to failure together with a reasonably high strain rate are highly desirable for superplastic forming capability [2,3]. In order to achieve these properties, the phases and grains are generally refined through the use of appropriate thermomechanical processing. The present research was initiated to examine, using Pb-Sn alloys as representative model materials, the potential for developing a new way of tuning the microstructure to achieve unprecedented superplastic properties.

Although there are numerous reports documenting superplastic properties in the Pb-Sn eutectic alloy, a review of the available data shows that true superplastic flow is rarely achieved upon testing at RT at a strain rate of 1.0×10^{-3} s^{-1}. The only true superplasticity in the eutectic alloy at a strain rate of 1.0×10^{-3} s^{-1} at RT is 600% in an extruded alloy [6] and 430% in an alloy processed by high-pressure torsion (HPT) [7]. In addition, an elongation of >2000% was reported at RT when using a very slow strain rate of 6.6×10^{-5} s^{-1} [4] and there was evidence that the elongation may be increased by introducing pre-straining [5].

The conventional approach for promoting superplasticity is to introduce deformation-induced grain refinement using, for example, rolling or extrusion of the as-cast eutectic alloy. However, these procedures have resulted in only marginal improvements in superplasticity of the Pb-Sn eutectic alloy at reasonably high strain rates at RT [7-10]. This situation arises because 1) the processing strain reached in these procedures is limited by the sample dimensional reduction and 2) the strain path for such normal-strain dominated processing is not effective, in comparison to other shear-strain dominated processing [11-13]. Other shear-strain dominated severe plastic deformation (SPD) approaches, such as equal-channel angular pressing (ECAP) [14] and HPT [15], are more suitable but nevertheless have yet to enable very high tensile elongations at RT at a strain rate of ~10^{-3} s^{-1}.

Recognizing this status quo, the present research exploits shear-dominated tube high-pressure shearing (*t*-HPS) which is an SPD technique described earlier [16,17] that provides the capability to mechanically mix Pb and Sn and thereby to form patterned phase domains with a grain size down to about one micrometer. This has the advantage of elevating superplasticity to a level that was not previously realized in Pb-Sn alloys at RT. In the *t*-HPS technique a very large shear strain is imposed and a bulk alloy is achieved in a single step. Compositional excursions in cast hypoeutectic alloys, caused by the pre-eutectic primary phase [18], are effectively avoided in this fully solid-state processing, thereby bypassing solidification altogether. Thus, it becomes possible to explore various alloy compositions, by producing a uniform microstructure with homogeneously distributed α (Pb rich) and β (Sn rich) phases/grains in order to search for the desired mix, in terms of the proportion of the two phases, the grain sizes and their overall spatial distributions, that optimize the superplastic behavior.

The experiments conducted in this research used 99.995% purity lead and 99.999% purity tin as the starting materials. Two different alloy compositions of Pb-62% Sn and

Pb-40% Sn (both in weight percentage) were examined using the same processing technique. For comparison purposes, cast alloys were made by melting the Pb and Sn according to the desired compositions and then casting in a cylindrical mold 50 mm in diameter and 60 mm in height. The cast billets were further rolled to a final thickness of 2 mm at RT. The *t*-HPS samples were processed in a home-made facility depicted schematically in Fig. 1, where the tubular sample is radially confined between a mandrel and an outer cylinder. Specifically, for the *t*-HPS Pb-62 wt% Sn alloy (corresponding to a Pb to Sn volume ratio of 28:72) the 360° central-angle tube was composed of columns of Pb and Sn with fan-shaped cross sections of different central angles: thus, a Pb column with a central angle of 101° was assembled with an Sn column with a central angle of 259°. For the *t*-HPS Pb-40 wt% Sn alloy where the volume ratio is ~50/50, the central angles for the Pb and Sn columns were both ~180°.

The Pb/Sn combination tube was axially constrained by the pressure ring and radially constrained by the mandrel and the cylinder. Then a hydraulic pressure was imposed at either end of the pressure ring to introduce a 1.0 GPa hydrostatic pressure in the tube wall such that the frictional forces at the interfaces between the sample-mandrel and the sample-cylinder were sufficiently high to prevent local slip. By fixing the outer cylinder and rotating the mandrel, or vice versa, a simple shear strain is produced within the tube wall [16]. In the present work, tangential shearing of the tube was conducted by rotating the outer cylinder up to 40 turns or 50 turns (the equivalent true strain is ~1,600 and 2,000, respectively) for *t*-HPS Pb-40% Sn and *t*-HPS Pb-62% Sn, respectively, thereby ensuring adequate mechanical mixing between the Pb and Sn.

The mixing mechanism is discussed in more detail later.

The microstructures of the processed samples were examined using electron backscatter diffraction (EBSD) in an SU1050 tungsten filament gun scanning electron microscope (SEM). The EBSD samples were taken from the center of the as-cast billet, along the longitudinal section for the rolled sheet and in the annular cross-section from the middle section of the micro-duplex alloy tube after *t*-HPS. The equivalent diameters of the circular areas of the grains were taken as the grain size. The aspect ratio was taken as the ratio of the length of the grains along the rolling direction to that along the normal direction for the rolled samples, and the ratio of the length along the tube circumferential direction to that along the radial direction for the *t*-HPS samples.

Flat plate-shaped tensile specimens were used for tensile testing with all samples having a gauge length of 3 mm and cross-sectional areas of 2×2 mm^2. Specimens were machined directly from the as-cast billet and the rolled sheets. For the *t*-HPS Pb-62% Sn and *t*-HPS Pb-40% Sn alloys, the tubes were first cut into two parts vertically across their diameters and then flattened. In practice, the change in microstructure and properties due to this flattening operation was negligible because the flattening stain was very small compared with the strain introduced by the *t*-HPS processing. All tensile tests were then conducted at RT using a Shimadzu machine operating at a constant rate of cross-head displacement with an initial strain rate of 1.0×10^{-3} s^{-1}.

Figure 2 shows representative EBSD images comparing the as-cast, rolled and the *t*-HPS Pb-62% Sn and Pb-40% Sn alloys. The maps showing the two-phase microstructures are displayed in panels a through f with the α phase in red and the β

phase in blue, whereas the corresponding orientation maps showing the reconstructed grain structures are given in g through l. For the as-cast Pb-62% Sn billet, the α phase had an average grain size of ~2.3 μm but the grains were dispersed within large β dendrites consisting of grains with a wide size distribution ranging from a few to several hundreds of micrometers. These latter large β grains were far outnumbered by the smaller grains, leading to an average Sn grain size of ~3.6 μm. A similar microstructure with a smaller average grain size of ~1.6 μm was observed in the as-cast Pb-40% Sn billet. Rolling produced a nearly equiaxed and uniformly distributed grain structure for both α and β but the average grain size remained of the order of a few micrometers. By contrast, the domains of the two phases in the Pb-Sn alloys processed by *t*-HPS were more uniformly distributed and the grains were more equiaxed and well refined.

For the alloys produced via *t*-HPS, the α/β phase volume ratio, average grain sizes and aspect ratios were 28.3/71.7, 1.1 μm and 1.14 for the Pb-62% Sn alloy by comparison with 49.7/50.3, 1.0 μm and 1.05 for the Pb-40% Sn alloy. Thus, the latter alloy is characterized by an equal volume fraction of the α and β phases, in addition to the micrometer grain size and equiaxed grain shape. These characteristics are expected to be beneficial for the occurrence of grain boundary sliding in superplasticity [1]. Table 1 summarizes and compares the measured phase ratios, average grain sizes and aspect ratios.

The RT engineering stress-strain curves are given in Fig. 3, together with insets showing the specimens after fracture. All tests were conducted at the initial strain rate of 1.0×10^{-3} s^{-1} and Table 2 summarizes the tensile properties of the alloys. As expected, the as-cast Pb-62% Sn and Pb-40% Sn alloys were not superplastic although rolling increased the elongation of the Pb-62% Sn alloy to almost ~200%. These elongations are generally consistent with published data for rolled and even ECAP samples [8,9,19].

By contrast, the *t*-HPS Pb-40% Sn and *t*-HPS Pb-62% Sn alloys exhibited excellent superplasticity at RT. The elongation of *t*-HPS Pb-62% Sn was 670% which corresponds to the highest room temperature superplastic elongation of the eutectic alloy using an initial strain rate of about 1×10^{-3} s^{-1} when the alloy was produced via casting and extrusion [6]. This was achieved because of the nearly equiaxed configuration of the grains as documented in Table 1 and the small grain size which facilitated sliding at the grain boundaries and interphase interfaces [20-22]. However, it is important to highlight that the elongation of the *t*-HPS Pb-40% Sn alloy is as high as ~1870%, which is a very significant advance over the elongation of ~670% recorded for the *t*-HPS Pb-62% Sn alloy.

Table 3 provides a summary of published data for the tensile elongations achieved in Pb-Sn alloys at RT measured at or near an initial strain rate of 1.0×10^{-3} s^{-1}. [6-10,19,23], It is readily apparent that, despite the use of several different post-casting procedures, no earlier experiments achieved elongations above a maximum of 600%. By contrast, the present *t*-HPS Pb-40% Sn alloy exhibited an exceptional elongation of ~1870% which exceeds earlier attempts by more than a factor of three.

The difference in behavior between the two alloys arises because, while the microstructures of the *t*-HPS Pb-40% Sn and *t*-HPS Pb-62% Sn alloys look similar, there is a major difference in their phase ratios. It is not by accident that superplasticty was first discovered in dual phase alloys since this is convenient for meeting the microstructural requirements for superplastic flow. Although the grain aspect ratio, phase contiguity ratio, boundary length of interfaces, interface segregation and boundary features are all important microstructural parameters governing superplasticity, a fine grain size is the most essential, and this is especially favored by the presence of two separate phases leading to retarded growth of the phase domains [22,24]. This suppression of coarsening is most effective with alloys having equal volumes of the two phases since this produces the maximum separation between the two phases [22].

This view is supported by the microstructural observation of interrupted tensile testing samples, as shown in Fig. 4. The average grain size after elongation to 600% of the *t*-HPS Pb-62% Sn alloy samples was estimated to be 2.4 ± 0.1 μm, and that of the Pb-40% Sn alloy tensile tested to an elongation of 1200% as 2.5 ± 0.1 μm. This shows that a fine grain structure is retained during tensile deformation, especially in the latter case with equal phase volume fractions.

Assume that phase coarsening during superplasticity follows the general kinetic relationship as that of conventional static annealing [25]: $d^n - d_0^n = Kt$, where d_0 and d are the phase/grain size at the start and time t, respectively, n is the grain growth exponent, and K the grain growth constant. Taking n=4 [26], the initial grain size from Table 1 and the grain size observed in interrupted tensile testing samples given above, K can be estimated as 5.3×10^{-3} and 3.2×10^{-3} $\mu m^4/s$ for Pb-62% Sn and Pb-40% Sn, respectively. This reduction in K, going from the Pb-Sn at eutectic composition to the equal volume fraction alloy, suggests that grain growth is retarded by increased heterogeneous interfaces when using equal volumes of the two phases. The thermally-induced growth of the phase domains is not favorable at the interphase boundaries as the two elements exhibit a positive heat of mixing. In addition, adjusting the phase ratio to ~50/50 maximizes the boundaries between mutually repulsive phase domains. Such chemically weakened boundaries are more conducive to grain boundary sliding and hence to superplastic flow [27].

The present unusual superplasticity results were obtained through processing using the tube high-pressure shearing technique and it is important therefore to examine and explain the mechanism and advantage of using this *t*-HPS procedure. The eutectic Pb and Sn system, characterized by a positive heat of mixing, is mechanically alloyed in the bulk solid state enabled by the SPD process in *t*-HPS. Mass transport is carried by a shearing or dislocation-forced relocation of atoms as in a ballistic process randomizing the redistribution of the elemental atoms. This externally driven intermixing proceeds towards uniformity but is effectively counter-balanced by a thermodynamically-biased diffusion which, for the Pb-Sn system, is the tendency to separate phases into a two-phase mixture. Steady-state is ultimately established as a self-patterned microstructure which, for the Pb-Sn alloys, corresponds to a two-phase mixture on a micrometer scale. A detailed analysis of the mechanisms of such compositional patterning is beyond the scope of this report but comprehensive details on phase/microstructure evolution in driven alloys are available elsewhere [28-30].

One advantage of preparing alloys using *t*-HPS is that it directly overcomes the metallurgical features dictated through ingot casting, including the formation and growth of dendrites, the segregation of alloying elements and the inherent coarsening of the microstructure. This is attractive in the present research where the objective is to refine and homogenize the distribution of the two grains/phases and thereby to form interphase boundaries that will facilitate superplasticity. With Pb-Sn providing an excellent example of this approach, it is reasonable to anticipate that processing by *t*-HPS will be similarly advantageous in other alloy systems where highly refined microstructures are difficult to produce using conventional casting.

In summary, the present results demonstrate that the solid-state synthesis of Pb-Sn alloys from bulk Pb and Sn via t-HPS processing is especially advantageous in reaching a phase structure different from that in conventional metallurgical casting. The Pb-40% Sn alloy in this investigation gave an exceptional elongation to failure of ~1870% at RT at an initial strain rate of 1.0×10^{-3} s^{-1}. This unprecedented superplasticity was achieved because *t*-HPS was able to produce, at an overall composition far-off the eutectic composition, homogenously mixed domains of Pb and Sn in nearly equal proportions, in addition to uniform equiaxed grains of about one micrometer in size. This provides the most effective stabilization of fine grains and promotes sliding at grain/interphase boundaries, boosting the chances for reaching unusual superplastic properties.

Acknowledgements

This work was supported by the National Key R&D Program of China (Grant No. 2017YFA0204403) and the National Natural Science Foundation of China (Grant No. 52074160). E.M. acknowledges XJTU for hosting his work at the Center for Alloy Innovation and Design (CAID). T.G.L. was supported by the European Research Council under Grant Agreement No. 267464-SPDMETALS. The EBSD experiments were performed at the Materials Characterization and Research Center of Nanjing University of Science and Technology.

References

[1] T.G. Langdon, J. Mater. Sci. 44 (2009) 5998-6010.

[2] K. Higashi, Japan, Mater. Sci. Tech. 16 (2000) 1320-1328.

[3] A.J. Barnes, J. Mater. Eng. Perform. 22 (2013) 2935-2949.

[4] M.M.I. Ahmed, T.G. Langdon, J. Mater. Sci. 18 (1983) 2407-2413.

[5] M.M.I. Ahmed, T.G. Langdon, J. Mater. Sci. 18 (1983) 3535-3542.

[6] T.K. Ha, Y.W. Chang, Mater. Sci. Forum, 357-359 (2001) 159-164.

[7] N.X. Zhang, M. Kawasaki, Y. Huang, T.G. Langdon, J. Mater. Metall. 14 (2015) 255-304.

[8] M.M.I. Ahmed, T.G. Langdon, J. Mater. Sci. Lett. 2 (1983) 59-62.

[9] M.M.I. Ahmed, T.G. Langdon, J. Mater. Sci. Lett. 2 (1983) 337-340.

[10] M.S. Soliman, Scripta Metall. Mater. 33 (1995) 919-924.

[11] V.M. Segal, Mater. Sci. Eng. A 338 (2002) 331-344.

[12] V. Segal, Materials, 11 (2018) 1175-1203.

[13] E. Bagherpour, N. Pardis, M. Reihanian, R. Ebrahimi, Int. J. Adv. Manuf. Technol. 100 (2019) 1647-1694.

[14] R.Z. Valiev, T.G. Langdon, Prog. Mater. Sci. 51 (2006) 881-981.

[15] A. Zhilyaev, T.G. Langdon, Prog. Mater. Sci. 53 (2008) 893-979.

[16] J.T. Wang, Z. Li, J. Wang, T.G. Langdon, Scripta Mater. 67 (2012) 810-813.

[17] Z. Li, P.F. Zhang, H. Yuan, K. Lin, Y. Liu, D.L. Yin, J.T. Wang, T.G. Langdon, Mater. Sci. Eng. A 658 (2016) 367-375.

[18] D.R. Askland, W.J. Wright. The Science and Engineering of Materials, Cengage

Learning, seventh ed., (2014) 394-401.

[19] E.A. El-Danaf, K.A. Khalil, M.S. Soliman, Mater Des. 34 (2012) 235-241.

[20] R.B. Vastava, T.G. Langdon, Acta Metall. 27 (1979) 251-257.

[21] M. Kawasaki, T.G. Langdon, J. Mater. Sci. 42 (2007) 1782-1796.

[22] M. Kawasaki, T.G. Langdon, J. Mater. Sci. 48 (2013) 4730-4741.

[23] L.P. Lugon, R.B. Figueiredo, P.R. Cetlin, J. Mater. Sci. Technol. 3 (2014) 327-330.

[24] T.G. Langdon, Metall. Trans. 13A (1982) 689-701.

[25] O.N. Senkov and M.M. Myshlyaev, Acta Metall. 34 (1986) 97-106.

[26] J.Kang, H.Conrad, Journal of Electronic Materials, 2001, 30(10):1303-1307.

[27] F. Cao, J. Cui, J. Wen, L. Fang, Journal of Materials Science & Technology, 16(2000) 55-58.

[28] R.S. Averback, P. Bellon, S.J. Dillon, J. Nucl. Mater. 553 (2021) 153015.

[29] D. Schwen, M. Wang, R.S. Averback, P. Bellon, J. Mater. Res. 28 (2013) 2687-2693.

[30] B. Stumphy, S.W. Chee, N.Q. Vo, R.S. Averback, P. Bellon, M. Ghafari, J. Nucl. Mater. 453 (2014) 66-74.

List of figures:

List of tables:

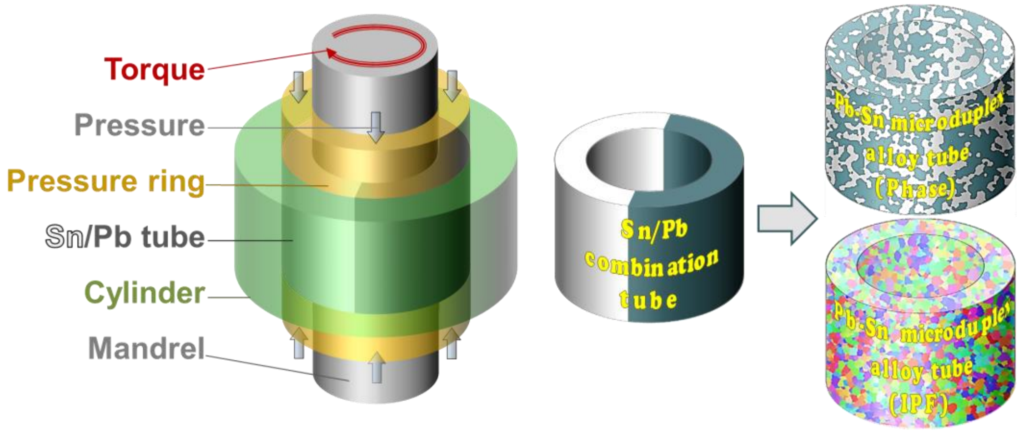

Fig. 1. Schematic illustration of the *t*-HPS setup (left). The Sn/Pb combination tube (middle) is processed into a Pb-Sn micro-duplex alloy tube with micrometer-scale phase domains/grains (right) in a single step of *t*-HPS processing.

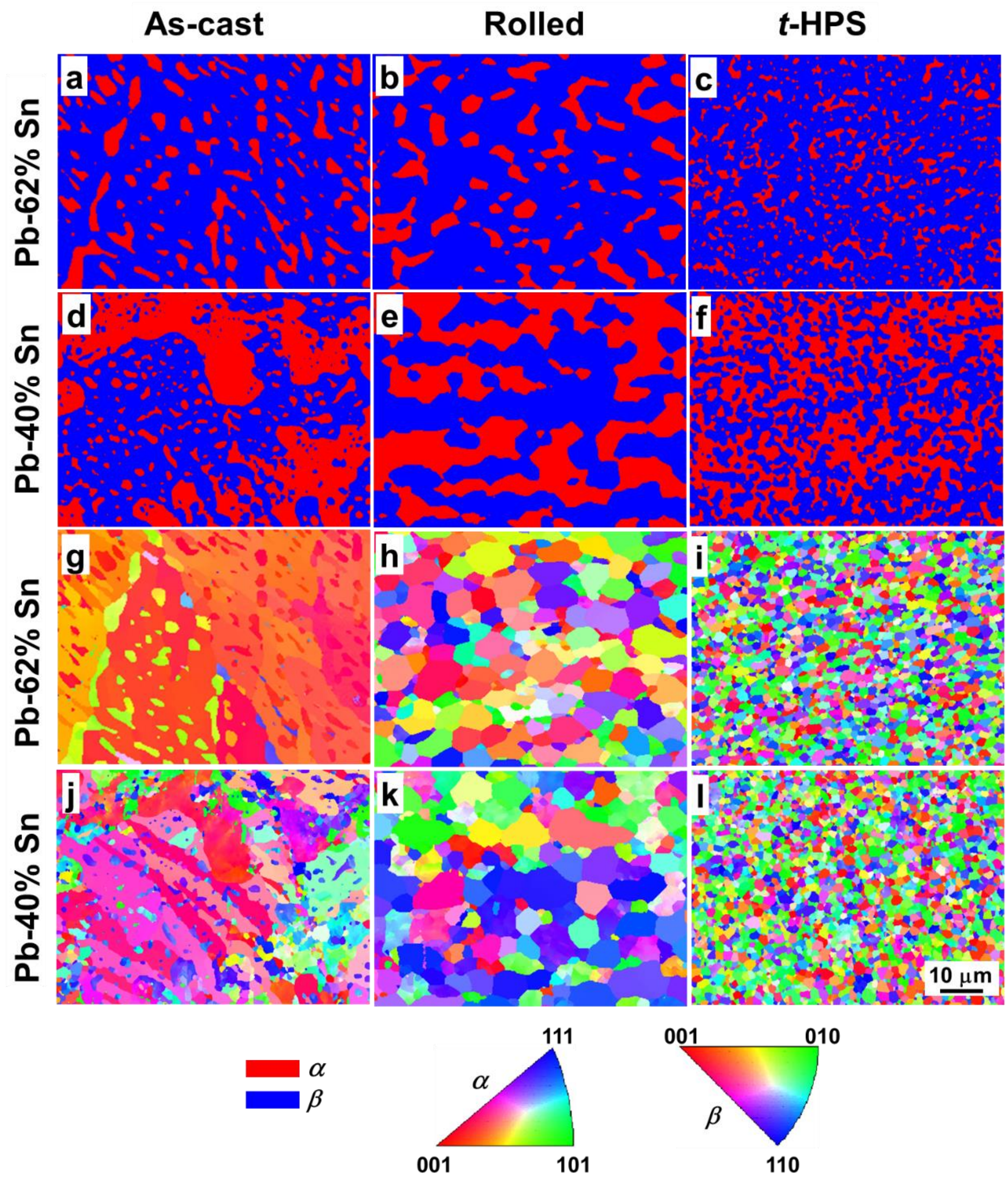

Fig. 2. EBSD images of cast, rolled and *t*-HPS Pb-62% Sn and Pb-40% Sn samples (a-f) with colors corresponding to α (red) and β (blue) (top); the corresponding orientation maps of grain structure (g-l) with colors corresponding to the various orientations in the stereographic triangles (bottom).

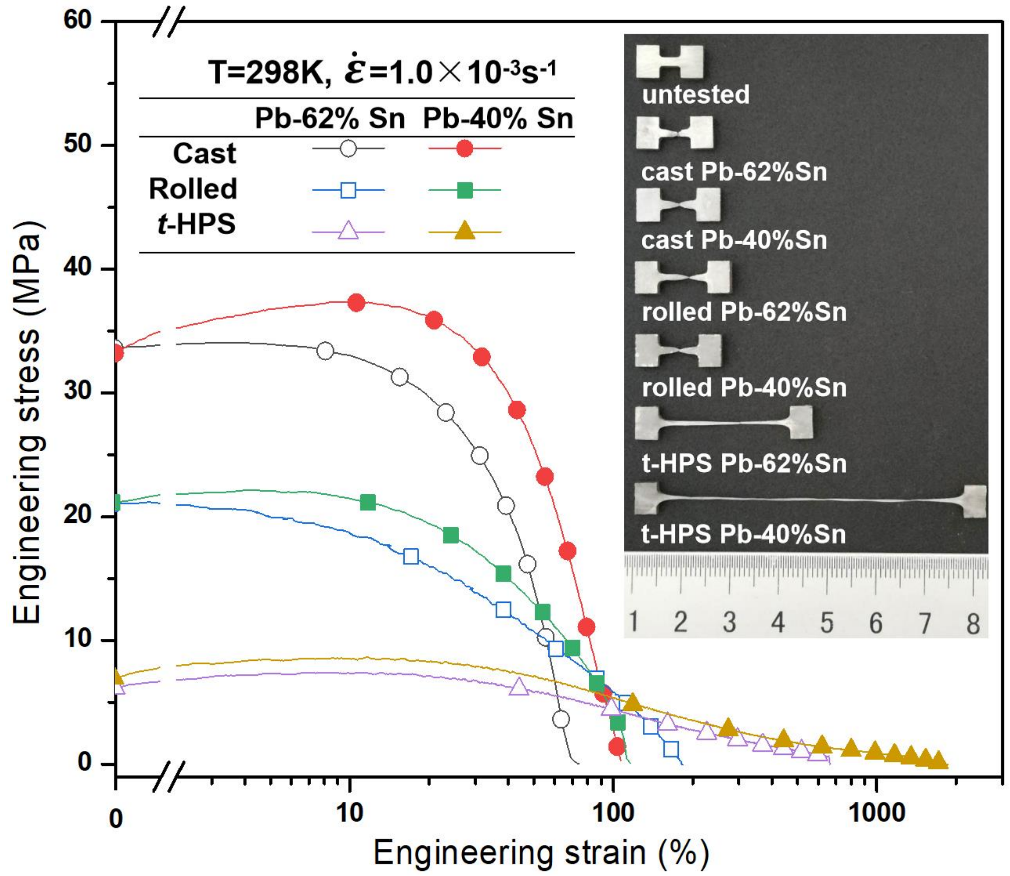

Fig. 3. Engineering stress-strain curves for the Pb-Sn alloys tested at the initial strain rate of 1.0×10^{-3} s^{-1} at RT: the inset shows the appearance of the specimens after pulling to failure, starting from the untested condition.

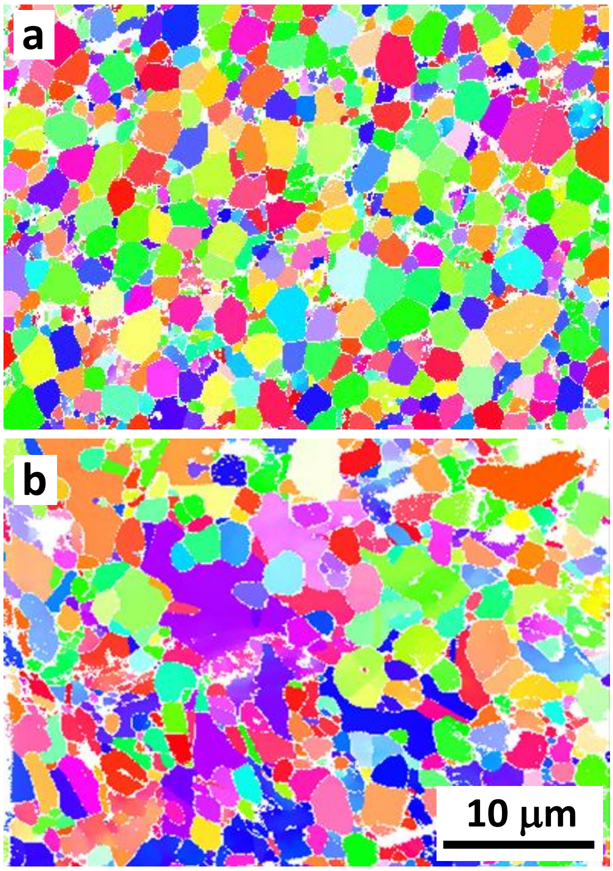

Fig. 4. Typical EBSD orientation maps observed on cross-section of t-HPS alloys (a) Pb-62% Sn tensile tested to elongation of 600%, and (b) Pb-40% Sn tensile tested to elongation of 1200%. Orientation legends are the same as those in Fig. 2.

Table 1 Measured phase ratios, grain sizes and aspect ratios in the Pb-Sn alloys

Sample	Phase ratio α/β	Average grain size (μm)			Grain aspect ratio		
		α & β	α	β	α & β	α	β
Pb-62% Sn Cast	/	2.6±0.2	2.3±0.1	3.6±0.3	/	/	/
Pb-62% Sn Rolled	27.2/72.8	3.1±0.1	2.0±0.1	4.8±0.2	1.51±0.02	1.57±0.04	1.42±0.04
Pb-62% Sn *t*-HPS	28.3/71.7	1.1±0.1	0.7±0.1	1.4±0.1	1.14±0.02	0.94±0.02	1.29±0.02
Pb-40% Sn Cast	/	1.2±0.1	1.0±0.1	1.6±0.2	/	/	/
Pb-40% Sn Rolled	51.0/49.0	2.7±0.1	1.8±0.1	5.4±0.2	1.29±0.02	1.27±0.02	1.32±0.04
Pb-40% Sn *t*-HPS	49.7/50.3	1.0±0.1	0.8±0.1	1.4±0.2	1.05±0.01	1.02±0.01	1.10±0.01

Table 2 Tensile properties of the Pb-Sn alloys at an initial strain rate of 1.0×10^{-3} s^{-1} at RT.

Sample	Peak stress (MPa)	Elongation (%)
Pb-62% Sn Cast	34.1	~74
Pb-62% Sn Rolled	21.2	~184
Pb-62% Sn *t*-HPS	7.4	~670
Pb-40% Sn Cast	37.4	~107
Pb-40% Sn Rolled	22.1	~116
Pb-40% Sn *t*-HPS	8.6	~1870

Table 3 Processing condition and properties of Pb-Sn alloys at or near an initial strain rate of 1.0×10^{-3} s^{-1} at RT [6-10,19,23].

Sample	Average grain size (μm)	Testing strain rate (s^{-1})	Elongation (%)	Reference
Pb-62% Sn Rolled	6.1	6.6×10^{-4}	200	Ahmed and Langdon [8]
Pb-62% Sn Rolled	3.3	6.6×10^{-4}	125	Ahmed and Langdon [9]
Pb-62% Sn Extruded	2.2	6×10^{-4}	320	Soliman [10]
Pb-40% Sn Extruded	/	1×10^{-3}	400	Ha and Chang [6]
Pb-62% Sn Extruded	2.5	1×10^{-3}	600	Ha and Chang [6]
Pb-80% Sn Extruded	/	1×10^{-3}	260	Ha and Chang [6]
Pb-62% Sn ECAP	6	1×10^{-3}	180	El-Danaf *et al.* [19]
Pb-62% Sn ECAP+roll	5.9	1×10^{-3}	60	Lugon *et al.* [23]
Pb-62% Sn HPT	3.3	1×10^{-3}	430	Zhang *et al.* [7]
Pb-62% Sn *t*-HPS	1.1	1×10^{-3}	~670	This work
Pb-40% Sn *t*-HPS	1.0	1×10^{-3}	~1870	This work